Kinetic Modeling of Hemicellulose Hydrolysis in the Presence of Homogeneous and Heterogeneous Catalysts

Tapio Salmi, Dmitry Yu. Murzin, Päivi Mäki-Arvela, Bright Kusema, Bjarne Holmbom, and Stefan Willför
Dept. of Chemical Engineering, Process Chemistry Centre, Åbo Akademi University, FI-20500 Turku/Åbo, Finland

Johan Wärnå
Dept. of Chemistry, Technical Chemistry, Chemical-Biological Center, Umeå University, SE-90187 Umeå, Sweden

DOI 10.1002/aic.14311
Published online January 16, 2014 in Wiley Online Library (wileyonlinelibrary.com)

Kinetic models were developed for the hydrolysis of O-acetyl-galactoglucomannan (GGM), a hemicellulose appearing in coniferous trees. Homogeneous and heterogeneous acid catalysts hydrolyze GGM at about 90°C to the monomeric sugars galactose, glucose, and mannose. In the presence of homogeneous catalysts, such as HCl, H_2SO_4, oxalic acid, and trifluoroacetic acid, the hydrolysis process shows a regular kinetic behavior, while a prominent autocatalytic effect was observed in the presence of heterogeneous cation-exchange catalysts, Amberlyst 15 and Smopex 101. The kinetic models proposed were based on the reactivities of the nonhydrolyzed sugar units and the increase of the rate constant (for heterogeneous catalysts) as the reaction progresses and the degree of polymerization decreases. General kinetic models were derived and special cases of them were considered in detail, by deriving analytical solutions for product distributions. The kinetic parameters, describing the autocatalytic effect were determined by nonlinear regression analysis. The kinetic model described very well the overall kinetics, as well as the product distribution in the hydrolysis of water soluble GGM by homogeneous and heterogeneous catalysts. The modelling principles developed in the work can be in principle applied to hydrolysis of similar hemicelluloses as well as starch and cellulose. *AIChE J*, 60: 1066–1077, 2014
Keywords: hemicellulose hydrolysis, kinetics, mechanism, autocatalysis, homogeneous catalyst, heterogeneous catalyst

Introduction

Hemicelluloses are valuable components in plant materials, such as wood and reed. Typical hemicelluloses appearing in the softwood and hardwood in the northern hemisphere are arabinogalactan, galactoglucomannan, and glucuronoxylan. Hemicelluloses can be obtained as side-products from the Kraft pulping process, but, in chemical sense, better through hot-water extraction of wood powder or wood chips. The extracted fractions can be used as such as thickeners, as additives in paints, glues, and alimentary products. The sugar monomers obtained from hemicelluloses have a large perspective of use, as such or as starting molecules for valuable chemicals. For instance, xylose obtained from arabinoglucuronxylane can be hydrogenated to xylitol, a valuable natural sweetener, anticaries, and anti-inflammatory agent. Mannose is known to suppress the symptoms of urinary track diseases. In general, sugar monomers and their hydrogenation products have anticaries and anti-inflammatory effects.[1]

In the world-wide transformation to the use of renewable raw materials, the monomeric sugars originating from hemicelluloses have a great potential in the preparation of platform chemicals for the chemical industry. A typical example is levulinic acid, which can be obtained from glucose through catalytic conversion.

The crucially important step in the utilization of hemicelluloses is the hydrolysis of the macromolecule to sugar monomers.[2,3] The hydrolysis can be performed with homogeneous or heterogeneous catalysts or with enzymes. The use of homogeneous catalysts is an option, as both organic and inorganic acids are known to catalyze the hydrolysis reaction. By optimizing the catalyst concentration and the reaction temperature, high conversions and monomer concentrations can be achieved, avoiding a further degradation of the monomers to low-molecular products.[1]

The catalyst separation is always an issue in homogeneous catalysis, as clean and efficient separation processes are still pretty expensive, and neutralization of the acid catalyst followed by precipitation is not a feasible technology, because it produces salts as stoichiometric coproducts. Heterogeneous catalysts could provide a very attractive alternative for the hydrolysis process of oligosaccharides,[4] hemicelluloses,[5,6] and even celluloses[7,8] provided that the reaction rate is high enough and the catalyst is durable. With heterogeneous catalysts, the catalyst separation problem is surmounted: larger catalyst particles can be placed in a fixed bed and suspended small particles used in slurry reactors can be separated by filtration. Hydrolysis of hemicelluloses with enzymes can be

Correspodence concerning this article should be addressed to D.Y. Murzin at dmurzin@abo.fi.

also viewed as heterogeneous catalysis if enzymes are immobilized on a solid matrix.[2,9,10]

In all cases, the experimental determination and mathematical modeling of the hemicellulose hydrolysis kinetics is of crucial importance. In this work, we present kinetic models for the hydrolysis of hemicelluloses in the presence of selected homogeneous and heterogeneous catalysts. A rational approach—instead of taking empirical pseudofirst-order models or pseudocomponents, such as "hemicellulose," "oligomer," or "monomer"—is to develop the kinetic concept on the concentrations of functional groups in the sugar units. In hemicellulose hydrolysis, the "functional groups" are the glycosidic bonds. The approach is similar to that applied to stagewise polymerization (polyesterification) and substitution of cellulose and starch.[11] Models based on this principle are applied in this article to the acid-catalyzed hydrolysis of galactoglucomannan, which appears in relatively large amounts (20–25%) in coniferous trees in the Northern hemisphere. The molecular structure is displayed in Figure 1.

Kinetic Phenomena and Reaction Mechanisms in the Presence of Homogeneous and Heterogeneous Catalysts

In spite that the hydrolysis of cellulose and hemicellulose has been studied quite a lot, as reviewed by Mäki-Arvela et al.,[1] quantitative investigations on the hemicellulose hydrolysis kinetics are quite few, and they are often based on a semiempirical approach, treating hemicellulose mixtures as one molecule. However, it has been shown for xylan hydrolysis, that xylan consists of rapid and slow-reacting fractions.[12,13] The portion of fast and slow fractions is determined by data fitting.[2] Application of this concept can explain the decrease of hydrolysis rate with conversion due to accumulation of a slow reaction fraction. Reactivity of hemicelluloses, comprising five-carbon sugars, was connected with the chemical structure of the polymer, having both internal and external xylooligosaccharide bonds.[2] In particular, it was demonstrated that in hydrolysis of xylooligosaccharides ranging between the dioligosaccharides and pentaoligosaccharides in dilute sulfuric acid one of the terminal bonds reacts 1.8 times faster than an internal bond.[14] Such difference in reactivity can explain increase of hydrolysis rate with decrease of degree of polymerization and subsequent increase in the number of terminal bonds. In most cases, pseudofirst-order kinetics with respect to the hemicellulose molecule is proposed.[15–17] The reaction order with respect to the acid concentration is generally proposed to be close to one. Some of the models take into account the formation of oligomers[16,18] with even different chain length,[19,20] whereas many models assume fast reactions of oligomers to monomers[2] thus omitting oligomers from kinetic considerations.[21]

In a recent study, Xu et al.[22] related the hydrolysis kinetics of *O*-acetyl-galactoglucomannan (GGM) to the change of molar mass. Kusema et al.[23] described the hydrolysis of arabinogalactan with the aid of unreacted arabinose and galactose groups in the polymer chain. The reaction was of first order with respect to the concentration of the glycosidic bond and the acid catalyst and the oligomers were neglected in the kinetic modelling, because their amounts were small.

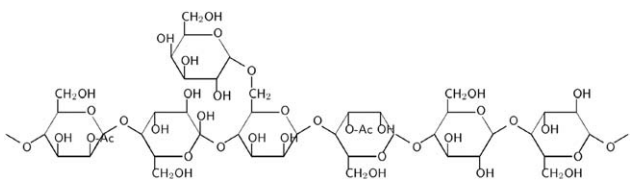

Figure 1. Molecular structure of *O*-acetyl-galactoglucomannan.

Due to relatively low temperature applied by Kusema et al.,[23] formation of such products as furfural and formic acid was not observed. Otherwise, concentration of arabinose will reach a maximum and then decrease. Contrary to pentoses, hexose monosaccharides, particularly glucose, are more resistant to chemical dehydration and the formation of aldehydes. In a recent publication,[24] the hydrolysis kinetics of GGM in the presence of several homogeneous catalysts (HCl, H_2SO_4, oxalic acid, trifluoroacetic acid, formic acid) and two heterogeneous catalysts (Amberlyst -15 and Smopex -101 with the acid capacity of 4.7 and 3.6 m_{eq}/g, respectively) was reported. The homogeneous catalysts represented both inorganic mineral acids and organic carboxylic acids, while the function of the heterogeneous catalysts was based on sulfonic acid groups fixed at a polymer matrix. The kinetic study revealed that organic and inorganic homogeneous acid catalysts behaved in a very similar manner, independent of the detailed chemical structure of the acid. No degradation products of the sugars, which are 5-hydroxymethylfurfural (HMF) from the hexoses, as well as further smaller degradation products were observed,[24] while they may in principle be formed during hydrolysis, if the reaction conditions become too severe due to high acid concentrations and high temperatures.

The kinetics of hemicelluloses hydrolysis, mainly comprising C5 sugars was based on schemes which include formation of decomposition products, in particular furfural.[12,25] Under mild conditions (e.g., low temperature and dilute mineral acid as a catalyst), xylose degradation is negligible.[25] In case of GGM under harsh conditions, formation of degradation products such as HMF and levulinic acid can be expected. In fact, it was reported that in case of hydrolytic hydrogenation of cellulose and hemicelluloses, which is conducted at about 170–200°C, such side products as HMF and furfural can be formed in substantial quantities.[26–29] This can further lead to coproduction of polymeric humans, which are formed during acid catalyzed conversion of hexoses with HMF[30] or through transformations of HMF first to 2,5-dioxo-6-hydrohexanal.[27] A recent kinetic model[31] for the hydrolysis of xylooligosaccharides to xylose by dicarboxylic acids in the temperature range 140–180°C included besides formation of xylose also generation of furfural and humins. It is worth noting that some diacids, such as maleic acid, could be different from mineral acids mimicking the selectivity of enzymes,[31] being both a proton donor and a proton acceptor. Maleic acid can even hydrolyze microcrystalline cellulose while preserving more of the monosaccharide as a sugar than sulfuric acid at equivalent conditions. Certain types of diacids[31] have thus an unusual property of preventing certain types of monosaccharides from being degraded to aldehydes.

No side products were formed in our experiments[24] as the reaction conditions were rather mild. The mass balance of the total organic carbon in the liquid-phase products was complete. Therefore, the formation of degradation products was not included in kinetic modeling.

The governing factor of the homogeneous acid catalysis turned out to be the acidity (pH) of the solution. It was proved that the rate of the homogeneous acid catalysis is

directly proportional to the concentrations of the hydroxonium ions (H_3O^+) being present in the solution. An analysis of the hydrolysis mixture by gel permeation chromatography (determination of the molecular mass distribution) revealed that the scission of the polymer chain is rather random and after a short induction period, the reaction rates decline with increasing reaction time and conversion.[24] The shapes of the kinetic curves suggest that the hydrolysis rate can be modeled with the aid of the concentrations of unreacted sugar units (galactose, glucose, mannose) in the reaction mixture. Acetyl groups in the hemicellulose are released in form of acetic acid during the hydrolysis, but their role is negligible, because acetic acid is a weak acid compared to the acid catalysts used in hydrolysis. The experimental evidence tells that the pH should be less than 1.5 to get hydrolysis rates of practical relevance under the experimental conditions discussed in the article. From the common organic acids, only oxalic acid ($pK_a = 1.23$), dichloroacetic acid ($pK_a = 1.29$), difluoroacetic acid ($pK_a = 1.24$), trichloroacetic acid ($pK_a = 0.08$), and trifluoroacetic acid ($pK_a = 0.26$) are strong enough to catalyze the hydrolysis within realistic reaction times. Even formic acid ($pK_a = 3.77$) is too weak to be used for hemicellulose hydrolysis in aqueous solutions under moderate temperatures used in our experiments. At elevated temperatures, significant hydrolysis of a hemicellolose from hard wood, that is, xylooligosaccharides, has been achieved in the presence of diacids with pK_a larger than 1.5.[31]

The mechanism of acid hydrolysis of β-glycosidic bonds in hemicelluloses is rather well-known. The main features of the mechanism are sketched in Figure 2. The acid dissociation step and the attachment of the hydroxonium ion to the glycosidic bond are rapid steps, while the C—O bond cleavage is the rate-limiting step, followed by rapid water addition. The degradation products, which could be prominent under more severe conditions, are not included in the figure, as they did not appear in our experiments. In our experiments, the feedstock, that is the purified hemicellulose was completely dissolved because of low concentrations.

The hydrolysis kinetics of GGM observed in the presence of heterogeneous and homogeneous catalysts was superficially very different. The initial reaction rate was much slower in the presence of the heterogeneous catalysts, but as the conversion increased and degree of polymerization decreased with time, the reaction was accelerated and an interesting autocatalytic behavior became visible: the kinetic curves took a parabolic form. A conventional interpretation of the kinetic curves could be based on the hypothesis of internal mass-transfer resistance in the pores of the heterogeneous catalyst. However, the heterogeneous catalyst with a substantial internal porosity (Amberlyst 15, styrene divinylbenzene sulphonated ion-exchange resin made of crosslinked spheres agglomerated together in a macroreticular-type structure with very large and very small pores) and the essentially nonporous catalyst (Smopex101, styrene sulfonic acid grafted polyolefin fiber) exhibited very similar autocatalytic behaviors. The initial molecular diffusion coefficient of GGM (DP $\approx$ 200) in an aqueous solution at 20°C is of the magnitude $D = 3 \times 10^{-11}$ m^2/s according to Wilke–Chang equation.[32] The effective diffusion coefficient ($D_e = (\varepsilon/\tau)D$) is much less, even according to an optimistic criterion only about 25% of the value of the molecular diffusion coefficient in aqueous environment. It should be noted that for the fiber catalyst (Smopex 101 of mean particle diameter 0.01 mm and the average length of 4 mm[33]), as well as for Amberlyst 15 with macropores controlled by degree of cross-linking no real pores exist to be penetrated. Thus, utilization of a classical approach to elucidate the influence of internal mass transfer by calculating molecular diffusion coefficients and evaluating effective diffusion coefficients might be questionable. In fact, such calculations based on the concept of catalyst effectiveness factor requiring estimations of effective diffusion coefficient give rather high values of effectiveness factor and minor influence of internal diffusion. On the other hand, higher-molecular-weight oligosaccharides would likely not easily penetrate the heterogeneous catalysts and configurational diffusion, similar to diffusion in zeolites, cannot be ruled out.

The reaction mechanism in the presence of heterogeneous catalysts could be sketched as follows. The hemicellulose molecule in the aqueous phase is far from linear, but it is branched and rolled to an almost spherical form at high molar masses (i.e., in the beginning of the reaction). Thus, the hydrolysis rate is determined by random collisions of the hemicellulose molecule with the acid sites at the outer surface of the heterogeneous catalyst. As the reaction progresses, the hemicellulose chain length decreases and the molecular structure becomes more open for encounters with sulfonic acid groups at the surface of the heterogeneous catalyst. In this way, the hemicellulose reactivity, the hydrolysis rate constants increase as the reaction proceeds and an autocatalytic effect appears in the kinetic curves. A scheme of the GGM hydrolysis process in the presence of a heterogeneous catalyst is displayed in Figure 3. Due to mild conditions (90°C) and negligible amounts of low-molecular degradation products when a hexose-based hemicellulose (GGM) is hydrolyzed, these compounds were not included in the

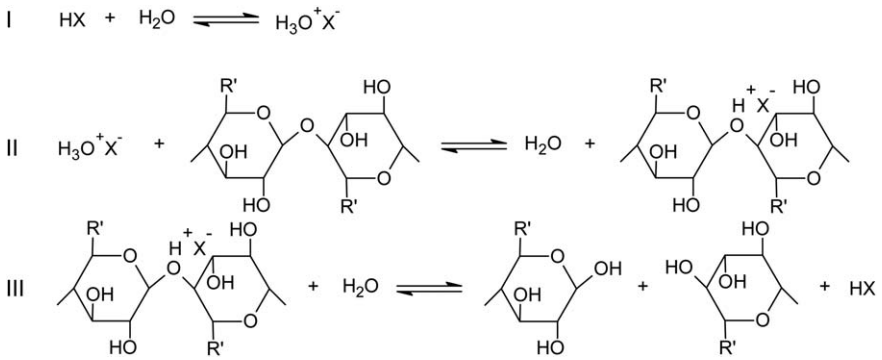

Figure 2. Homogeneous hydrolysis mechanism (R′ = CH_2OH).

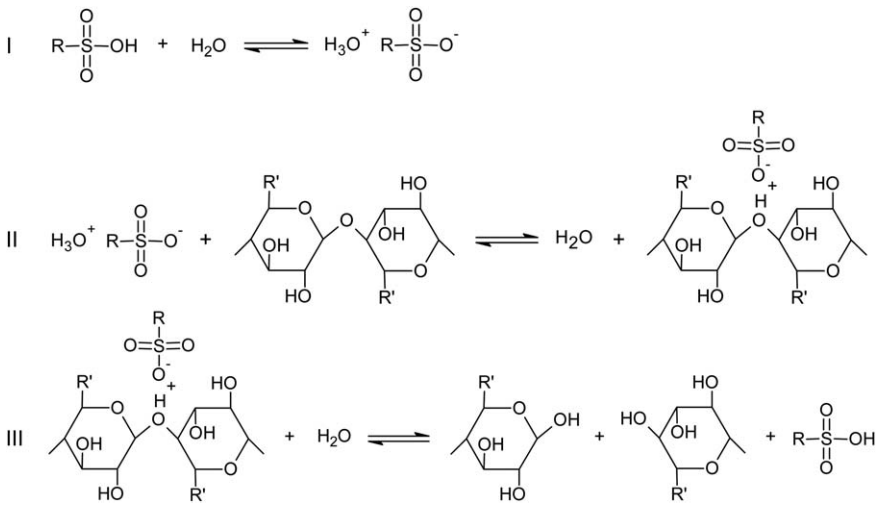

Figure 3. Heterogeneously catalyzed hydrolysis mechanism (R′ = CH_2OH).

model. Note that when the hydrolysis products are hexoses they show significantly lower degradation and formation of aldehydes than pentoses, which would be derived from xylan or arabinoxylan. Mechanisms of glucose degradation, which might be operative at more severe conditions, were reported in the literature.[34]

Experimental Methods and Procedures

GGM was isolated from thermomechanical pulp of Norway spruce (*Picea abies*) following a procedure reported previously.[35] The water extract was purified with filtration and ultrafiltration. Ethanol:water in a ratio of 4:1 was added to concentrated GGM solution to precipitate GGM, followed by drying. The GGM was further purified by redissolving it in water and performing dialysis. The average molar mass of GGM extracted from TMP process waters is around 20 kDa and the ratio of Gal:Glc:Man was equal to 0.5:1:4.[22] Weight-average and number-average molar mass (Mw and Mn) and molar mass distribution were determined by high-pressure size exclusion chromatography in online combination with a multiangle laser light scattering instrument and a refractive index detector. More details are given in the original article.[22]

The following homogeneous and heterogeneous catalysts were used: HCl, H_2SO_4, CF_3COOH, $(COOH)_2$, Amberlyst 15, and Smopex 101. Amberlyst 15 is an ion-exchange resin with particle diameters of 0.45–0.60 mm, whereas Smopex 101 is a fibrous resin catalyst, with the fiber diameter of 10 μm. The Amberlyst and Smopex catalysts had the acid capacities of 4.7 and 3.6 m_{eq}/g, respectively. The average pore size of Amberlyst 15 is 40–90 nm, while Smopex 101 is a nonporous catalyst made from polyethylene-grafted polystyrene. Sulfonic acid groups are the active sites of both catalysts. The acid loading of the homogeneous catalyst was varied to the corresponding pH values of 0.5, 1.0, and 1.5, whereas for the heterogeneous catalysts it was pH value 1.0, based on the concentration of the active sulfonic acid sites (c_H).

The kinetic experiments of GGM hydrolysis were carried out in a laboratory-scale jacketed glass reactor heated by silicon oil and equipped with an impeller stirrer. The liquid volume of the reactor was 100 mL. The reaction temperature was kept at 90°C and the initial concentration of GGM was 5g/l. Because the mass concentration of GGM was 5 g/L and about 111 glycosidic linkages are present in a polymer of 20 kDa, the concentration of the glycosidic bonds was more than three orders of magnitude lower than the water concentration (55.5 mol/L) and thus the concentration of water could in practice be assumed constant. The acid loading of the homogeneous catalyst was varied to the corresponding pH values of 0.5, 1.0, and 1.5, whereas for the heterogeneous catalysts it was pH value 1.0, based on the concentration of the active sulfonic acid sites (c_H).

In case of homogeneous catalysis, the liquid phase was preheated to the desired reaction temperature in few minutes, and the catalyst was added. The stirring impeller (800 rpm) was switched on. In case of heterogeneous catalysis, preheating of the substrate to about 50°C was done outside of the reactor under continuous agitation with a magnetic stirrer. The catalyst was placed in the reactor and heated up to about 70°C. Thereafter, the preheated substrate was introduced in the reactor and the temperature was then raised to the desired temperature under stirring which took few minuites. The temperature of the reaction mixture was kept thereafter constant (with the precision of 0.5°C).

Samples were withdrawn during the experiments and analyzed with gas chromatography. In this way, very precise kinetic curves were recorded. The details of the experimental procedure are described in the previous publication of our group.[24]

The pH of the filtrate was measured in several experiments with Smopex catalyst. It had the value of about 2.5. In fact, the pH was very stable after already 300 min, even if the autocatalytic behavior started to be pronounced much later. Therefore, the catalyst activity is attributed not to the liquid acid catalysis in case of solid acid catalysts even if leaching of sulfonic groups cannot be completely ruled out.

Kinetic Model for Homogeneous Catalysts

Mechanism and rate equation

The mechanism of the hydrolysis of starch, cellulose, and hemicelluloses in the presence of homogeneous catalysts is pretty well-known. Based on the mechanism sketched in Figure 2, the reaction steps of the hydrolysis can be written as

$$HX + H_2O = H_3OX \quad (I)$$

$$H_3OX + G0 = H_2O + HG0X \quad (II)$$

$$HG0X + H_2O \rightarrow P + Q + HX \quad (III)$$
$$G0 + H_2O \rightarrow P + Q$$

where HX is the acid catalyst, G0 is the glycosidic bond in mannose, galactose, or glucose, HG0X is an intermediate complex, and P and Q denote the product molecules. Steps I and II are rapid equilibria, while step III, involving the C—O bond cleavage is slower. Step III proceeds through a carbenium ion intermediate. The quasiequilibrium hypothesis is applied to Steps I and II, giving the concentration of HG0X, $c_{HG0X} = K_1K_2c_{HX}c_{G0}$. The rate of Step III is $r = k_3c_{HG0X}c_W = k_3K_1K_2c_{HX}c_Wc_{G0}$. The constants can be merged to $k = k_3K_1K_2$ giving $r = kc_{HX}c_Wc_{G0}$.

Kinetics in batch reactor

Based on the reasoning above, the formation rate of hydrolyzed mannose units in a constant-volume isothermal batch reactor can be expressed as

$$dc_M/dt = k_Mc_Hc_Wc_{M0} \quad (1)$$

where c_H, c_W, and c_{M0} denote the concentrations of the catalyst, water, and unhydrolyzed mannose units, respectively. The total concentration of mannose units remains constants, provided that now further degradation to low-molecular products takes place

$$c_{0M} = c_{M0} + c_M \quad (2)$$

from which the concentration of unsubstituted mannose units is solved and inserted in Eq. 1

$$dc_M/dt = k_Mc_Hc_W(c_{0M} - c_M) \quad (3)$$

Analogously, we can derive the balance equations for the formation of hydrolyzed galactose and glucose units

$$dc_{GA}/dt = k_{GA}c_Hc_W(c_{0GA} - c_{GA}) \quad (4)$$

$$dc_G/dt = k_Gc_Hc_W(c_{0G} - c_G) \quad (5)$$

The further treatment of Eqs. 3–5 depends on the initial concentration level of the hemicellulose. For high concentrations of the hemicellulose, the water consumption has to be taken into account. The reaction stoichiometry gives for a batch reactor the following condition

$$dc_W/dt = -(dc_G/dt + dc_{GA}/dt + dc_M/dt) \quad (6)$$

Integration of Eq. 6 gives

$$\int_{c0W}^{cW} dc_W = -\left(\int_0^{cG} dc_G + \int_0^{cGA} dc_{GA} + \int_0^{cM} dc_M\right) \quad (7)$$

resulting in the stoichiometric relationship

$$c_W = c_{0W} - (c_G + c_{GA} + c_M) \quad (8)$$

In case of dilute solutions of hemicelluloses, $c_{0W} >> c_G + c_{GA} + c_M$ and $c_w \approx c_{0W}$ during the reaction.

The relative product distribution can be calculated from Eqs. 3–5. Division of Eq. 3 by Eq. 4 gives

$$dc_M/dc_{GA} = (k_M/k_{GA})\frac{c_{0M} - c_M}{c_{0G} - c_G} \quad (9)$$

which implies that the relative product distribution is independent of the catalyst and water concentrations in all cases. Equation 9 can be solved by separation of the variables and integration

$$\int \frac{dc_M}{c_{0M} - c_M} = (k_M/k_{GA})\int \frac{dc_{GA}}{c_{0GA} - c_{GA}} \quad (10)$$

Integration with the limits $[0,c_M]$ and $[0,c_{GA}]$ gives

$$\ln(1 - c_M/c_{0M}) = (k_M/k_{GA})\ln(1 - c_{GA}/c_{0GA}) \quad (11)$$

Furthermore, it is recalled that the initial concentration of unhydrolyzed units (c_{0GA}, c_{0M}) are equal to the asymptotic concentrations of the monomers ($c_{\infty GA}$, $c_{\infty M}$ at $t \rightarrow \infty$), provided that complete hydrolysis is achieved and no side reactions take place.

Analogously, it can be derived for glucose and galactose

$$\ln(1 - c_G/c_{0G}) = (k_G/k_{GA})\ln(1 - c_{GA}/c_{0GA}) \quad (12)$$

The model can be tested by preparing the double logarithmic plots $\ln(1 - c_i/c_{0i})$ vs. $\ln(1 - c_{GA}/c_{0GA})$ (i = M or i = G). If the model is valid, the plots provide straight lines with the slopes k_i/k_{GA}. According to Eqs. 11 and 12, the concentrations of substituted units are related by

$$c_i/c_{0i} = 1 - (1 - c_{GA}/c_{0GA})^{k_i/k_{GA}} \quad (13)$$

where i = G or i = M.

Depending on the relative reactivities (k_i/k_{GA}), the curves representing Eq. 13 are either convex or concave; for the case that $k_i/k_{GA} = 1$, a straight line with the slope equal to 1 is obtained.

For the general case, when the water consumption is taken into account, the coupled differential equation system

$$dc_i/dt = k_ic_H\left(c_{0W} - \sum c_j\right)(c_{0i} - c_i) \quad (14)$$

is solved numerically for each group (i = G, GA, M and j = G,GA,M) to obtain the concentrations of the hydroxyl groups.

In case of diluted solutions, $c_{0W} >> \Sigma c_j$, and pseudofirst-order decoupled differential equations are obtained. They are easily solved analytically by separation of variables and inserting the limits $[0,t]$ and $[0,c_i]$. The result becomes

$$-\ln(1 - c_i/c_{0M}) = k_ic_Hc_{0W}t \quad (15)$$

that is

$$c_i/c_{0i} = 1 - \exp(-k''_it) \quad (16)$$

where $k''_i = k_ic_Hc_{0w}$. The model can be checked with a test plot of Eq. 15.

For pseudofirst-order kinetics, an overall rate constant (k') for the hydrolysis processes can be derived by adding the balance equations (i = G,GA,M)

$$-\sum \ln(1 - c_i/c_{0i}) = \left(\sum k_i\right)c_Hc_{0W}t \quad (17)$$

which implies that the overall rate constant $k' = \Sigma k_i$ can be determined by plotting the left-hand side vs. the reaction time. From the slope (ω) of the plot, the overall rate constant is obtained as follows

$$k' = \sum k_i = \frac{\omega}{c_Hc_{0W}} \quad (18)$$

The plots of the relative concentrations give the slopes $\alpha_1 = k_G/k_{GA}$ and $\alpha_2 = k_M/k_{GA}$ (Eqs. 11 and 12) and we get

$$k_{GA} = \frac{k'}{1+\alpha_1+\alpha_2} \tag{19}$$

$$k_G = \alpha_1 k_{GA} \quad k_M = \alpha_2 k_{GA} \tag{20}$$

This implies that the rate constants can be preliminary estimated from simple plots.

Modeling of Autocatalytic Kinetics over Heterogeneous Catalysts

Autocatalysis and degree of polymerization

The general reaction mechanism over heterogeneous acid catalysts is similar to that presented for homogeneous acid catalysts, but the proton comes from the sulfonic acid group of the heterogeneous acid catalyst. Thus, the same mechanism and rate equations, which were derived above for homogeneous catalysis can be used here, but the autocatalytic effect should be explained.

Provided that the autocatalytic effect observed in the presence of heterogeneous catalysts is caused by the change of the hemicellulose conformation as the chain length diminishes, the increasing reaction velocity can be interpreted as an increasing rate constant as the hydrolysis reaction proceeds.

Two variables are of particular importance in the description of hydrolysis kinetics, namely the overall conversion (X) and the degree of polymerization (DP). In the present case, the conversion can be described as follows

$$X = \frac{n_0 - n}{n_0} \tag{21}$$

where n_0 and n denote the number of glycosidic bonds in the beginning of the reaction ($t = 0$) and after some reaction time ($t > 0$), respectively. The degree of polymerization is DP_0 in the beginning and decreases toward DP, as the hydrolysis reaction progresses. DP_0 and DP are related to the number of glycosidic bonds by $DP_0 = n_0 + 1$ and $DP = n + 1$. This implies that DP is related to X by

$$X = \frac{DP_0 - DP}{DP_0 - 1} \tag{22}$$

In practice $X = 1 - DP/DP_0$ since $DP_0 >> 1$. In case of autocatalysis, the rate constant increases as DP decreases during the reaction. The simplest way to relate the increase of the rate constant to the decrease of DP is to use an explicit function based on an empirical differential equation. A reasonable Ansatz is

$$dk/dDP = -A' DP^{\gamma'} \tag{23}$$

which can be solved by separation of variables and integration with the limits $[k_0, k]$, $[DP_0, DP]$ and $[k_0, k_\infty]$, $[DP_0, 1]$. The result becomes

$$k - k_0 = \frac{A'}{\gamma'+1}\left({DP_0}^{\gamma'+1} - DP^{\gamma'+1}\right) \tag{24}$$

$$k_\infty - k_0 = \frac{A'}{\gamma'+1}\left({DP_0}^{\gamma'+1} - 1\right) \tag{25}$$

Combination of Eqs. 24 and 25 gives

$$k = k_0 + (k_\infty - k_0)\left(\frac{{DP_0}^{\gamma'+1} - DP^{\gamma'+1}}{{DP_0}^{\gamma'+1} - 1}\right) \tag{26}$$

Recalling that $DP_0 >> 1$, Eq. 26 can be rearranged to

$$k = k_0(1 + \beta'(1 - (DP/DP_0)^{\alpha'}) \tag{27}$$

where $\alpha' = \gamma' + 1$ and $\beta' = (k_\infty - k_0)/k_0$. In practice, the rate constant increases from k_0 toward $k_0(1 + \beta')$ as the reaction progresses. $DP/DP_0 \approx 1 - X$ (Eq. 22), which implies that

$$k = k_0(1 + \beta'(1 - (1 - X)^{\alpha'}) \tag{28}$$

Equation 28 reveals that the autocatalytic effect can be described by a simple two-parameter model, α' and β' being the adjustable parameters, which can be determined from experimental data by regression analysis.

Alternatively, the increase of the rate constant can be related directly to the conversion (X) by an empirical differential equation

$$dk/dX = AX^{\gamma} \tag{29}$$

where γ is an empirical exponent. If $\gamma = 1$, a linear increase of the rate constant is expected. The differential equation is solved from zero conversion ($X = 0$) to an arbitrary conversion (X), the corresponding values of the rate constants being k_0 and k. The result becomes

$$k - k_0 = \frac{A}{\gamma+1} X^{\gamma+1} \tag{30}$$

At complete conversion ($X = 1$) we get from Eq. 30 the limiting case

$$k_\infty - k_0 = \frac{A}{\gamma+1} \tag{31}$$

Combination of Eqs. 30 and 31 gives

$$k = k_0(1 + \beta X^{\alpha}) \tag{32}$$

where $\alpha = \gamma + 1$ and $\beta = (k_\infty - k_0)/k_0$. The principal behavior of the rate constant for different values of α and α' is illustrated by Figure 4. For the special case that $\alpha = \alpha' = 1$, the curves predicted by Eqs. 28 and 32 coincide. The values $\alpha = 0.5$ and $\alpha' = 2$ correspond to the case that the rate constant increases rapidly in the beginning of the reaction, while $\alpha = 2$ and $\alpha' = 0.5$ imply that the rate constant increases at high conversions.

If we presume that the rate constants for all of the hydrolysis processes change in a similar manner as a function of the overall conversion, Eq. 32 is rewritten to

$$k_j = k_{0j}(1 + \beta X^{\alpha}) \tag{33}$$

which de facto implies that $\beta = (k_{\infty j} - k_{0j})/k_{0j}$ is constant for all of the sugar units. If the minor amounts of oligomers formed during the initial stage of the reaction are neglected, the total conversion (X) can be calculated from the monomer products

$$X = \frac{c_{GA} + c_G + c_M}{c_{0GA} + c_{0G} + c_{0M}} = \frac{\sum c_j}{\sum c_{0j}} \tag{34}$$

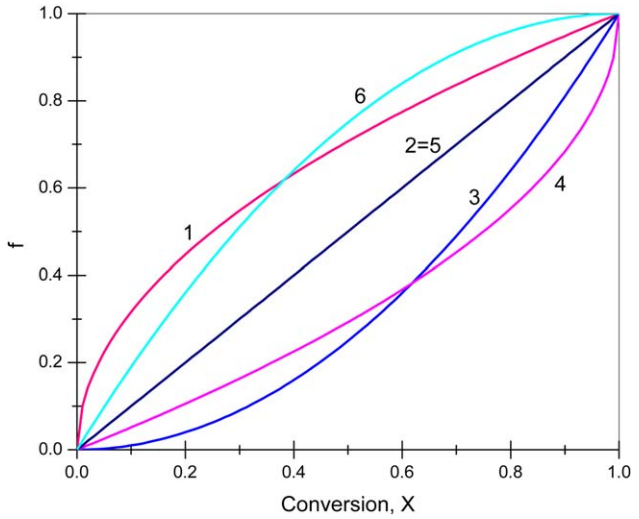

Figure 4. The behavior of functions $f = 1 - (1 - X)^{\alpha'}$ and $f = X^{\alpha}$, Eqs. 28 and 32.

The curve numbers represent the values of α and α': 1 ($\alpha = 0.5$), 2 ($\alpha = 1$), 3 ($\alpha = 2$), 4 ($\alpha' = 0.5$), 5 ($\alpha' = 1$), and 6 ($\alpha' = 2$). [Color figure can be viewed in the online issue, which is available at wileyonlinelibrary.com.]

Autocatalytic kinetics in batch reactor

The general balance equation for a substituted unit in an isothermal, constant-volume batch reactor, in the presence of a heterogeneous catalyst can be written as

$$dc_i/dt = k_i c_H c_W c_{i0} \rho_B \tag{35}$$

where ρ_B is the catalyst bulk density ($\rho_B = m_{cat}/V_L$). The following stoichiometric relations are inserted in Eq. 35

$$c_W = c_{0W} - \sum c_j \tag{36}$$

$$c_{i0} = c_{0i} - c_i \tag{37}$$

$$k_i = k_{0i}\left(1 + \beta\left(\frac{\sum c_j}{\sum c_{0j}}\right)^{\alpha}\right) \tag{38}$$

The balance equation becomes now

$$dc_i/dt = k_{0i}\left(1 + \beta\left(\frac{\sum c_j}{\sum c_{0j}}\right)^{\alpha}\right) c_H\left(c_{0W} - \sum c_j\right)(c_{0i} - c_i)\rho_B \tag{39}$$

The influence of the contributions is clearly visible from Eq. 39: the concentrations of water and unhydrolyzed units decrease with time, whereas the rate constant (k_i, Eq. 38) increases with increasing time (increasing conversion), reflecting the autocatalytic effect. For dilute solutions of hemicelluloses, the water concentration is practically constant.

In general, the model Eq. 39 is solved numerically for galactose, glucose, and mannose units and the parameters (k_{0G}, k_{0GA}, k_{0M}, α and β) are estimated by nonlinear regression analysis.

However, a first test of the model can be accomplished by considering the ratios of the balance equations. For instance, when the balance equations of glucose and mannose are divided by that of galactose, the result becomes

$$dc_G/dc_{GA} = (k_{0G}/k_{0GA})\frac{c_{0G} - c_G}{c_{0GA} - c_{GA}} \tag{40}$$

$$dc_M/dc_{GA} = (k_{0M}/k_{0GA})\frac{c_{0M} - c_M}{c_{0GA} - c_{GA}} \tag{41}$$

A comparison of Eqs. 40 and 41 with the corresponding Eq. 9 representing the homogeneous kinetics reveals that the equations have exactly the same mathematical structure, but k_i/k_{GA} is now replaced by k_{0i}/k_{0GA}. Thus, we can write the final relationship analogously with Eq. 13

$$c_i/c_{0i} = 1 - (1 - c_{GA}/c_{0GA})^{-k_{0i}/k_{0GA}} \tag{42}$$

where $i = G$ or $i = M$. A chemical interpretation can be given as follows. The relative reactivities for a heterogeneous catalyst depends on the initial values of the rate constants only, and the logarithmic plot

$$\ln(1 - c_i/c_{0i}) = (k_{0i}/k_{0GA})\ln(1 - c_{GA}/c_{0GA}) \tag{43}$$

is independent of the concentration of the active sulfonic acid sites (c_H) on the catalyst surface, the water concentration, and the catalyst amount. The relative reactivity is determined by the initial ratio of the rate constants solely, but this ratio might be temperature dependent, if the rate constants have different activation energies. The test of the theory presented above will be provided in the subsequent section.

In the use of nonpurified feedstock, the catalyst might deactivate, for example, through fouling. Catalyst fouling was not included in the model, as the GGM used in the experimental work was purified using filtration and ultrafiltration (see the section Experimental Methods and Procedures).

Estimation of kinetic parameters

The same parameter estimation strategy was used both for homogeneous and heterogeneous catalysts. First, the diagnostic double logarithmic plots, such as Eq. 43 were prepared to check the validity of the model; thereafter the kinetic parameters (k_{0i} and β) were estimated by nonlinear regression analysis.

In the estimation of the kinetic parameters, the residual sum of squares (Q) was minimized

$$Q = \sum_k \left(c_{iexp,t} - c_{i,t}\right)^2 \tag{44}$$

where "exp" refers to the experimental data and c_i (galactose, glucose, mannose) the concentrations predicted by the model. The initial concentrations were calculated backwards from the final concentrations of the released sugar monomers.

The underlying differential equations were solved by a backward difference method implemented in a stiff ordinary differential equation-solver during the parameter estimation. A Levenberg–Marquardt algorithm was used in the minimization of the objective function. The regression software Modest[36] was used in the computations. The results were checked by standard statistical analysis as well as by the degree of explanation (R^2) defined by

$$R^2 = 1 - \frac{\Sigma(c_{iexp,t} - c_{i,t})^2}{\Sigma(c_{iexp,t} - c_{iav,t})^2} \tag{45}$$

The degree of explanation compares the actual model with the simplest possible model, that is description of the data by average values of the concentrations.

Modeling Results and Discussion

The primary kinetic data recorded for the homogeneous catalysts (HCl, pH = 0.5–1.5 and other acids) are presented in Figure 5, and the data obtained for the heterogeneous catalysts (Smopex 101 and Amberlyst 15) are displayed in Figure 6. As revealed by the figures, the behavior of the system changes very much, as the heterogeneous catalyst is introduced: the hydrolysis rate is slower, but autocatalysis becomes visible. At the highest pH, the lowest acid concentration, some autocatalytic effect is also visible for HCl (Figure 5), the main reason for this might be the formation of oligomers in the beginning of the reaction.

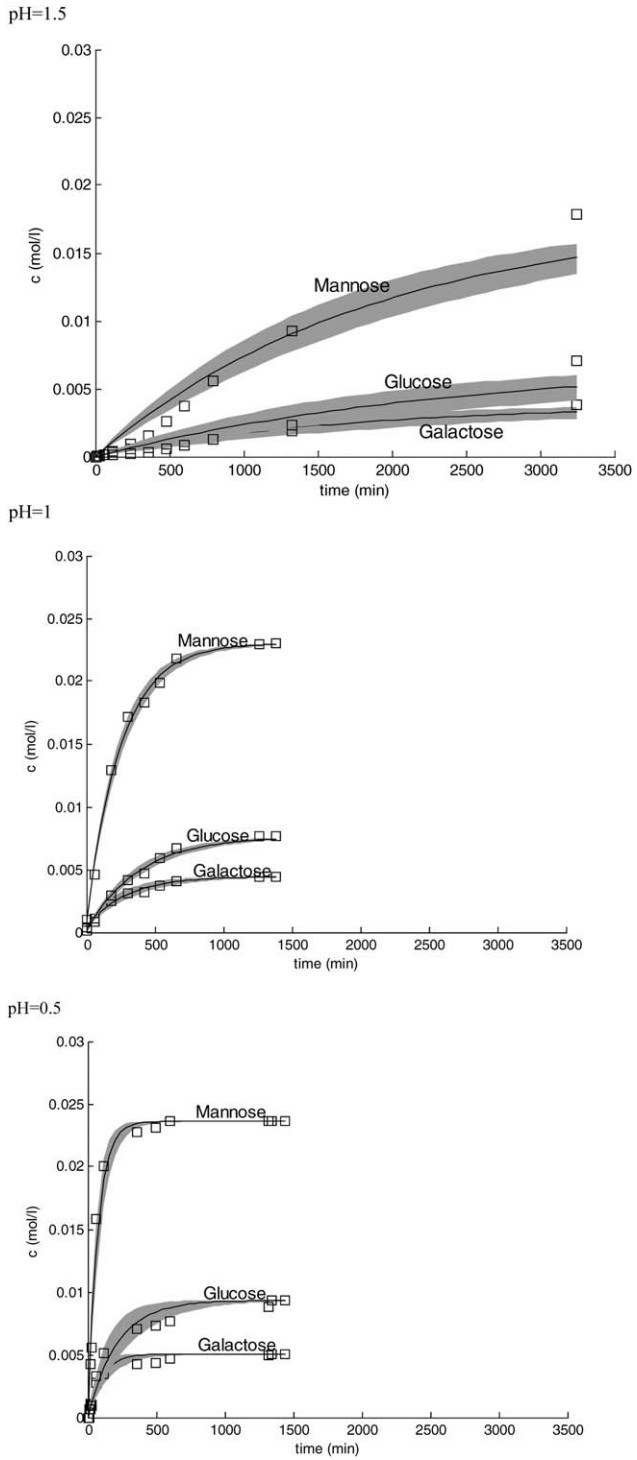

Figure 5. Hydrolysis kinetics of GGM.

Lines represent the model prediction: mannose (blue), glucose (red), and galactose (green). Conditions: T = 90°C, catalyst:HCl.

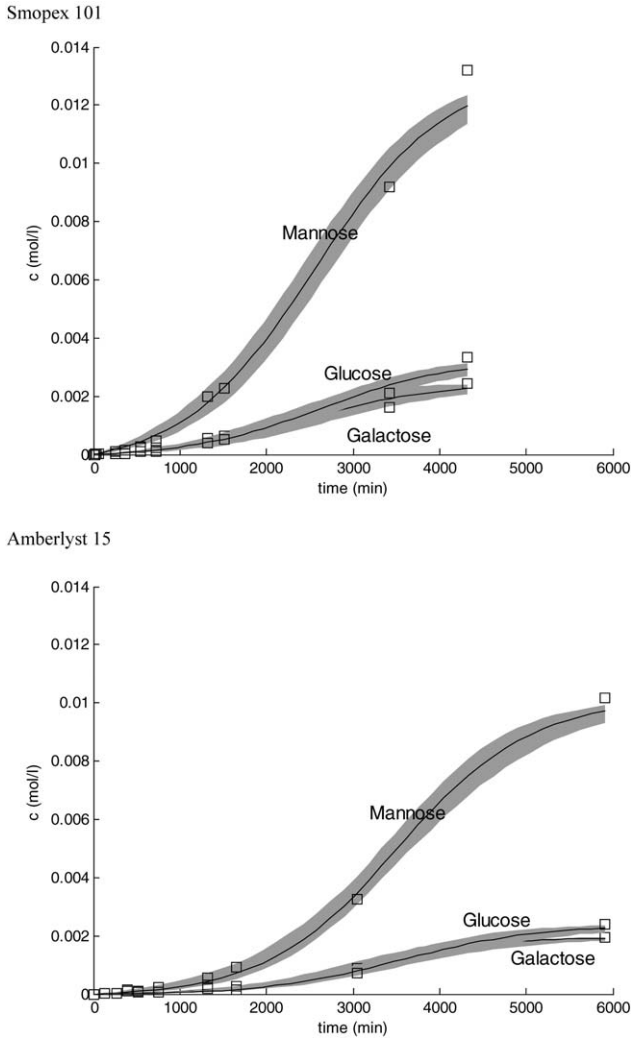

Figure 6. Hydrolysis kinetics of GGM.

Lines represent the model prediction: mannose (blue), glucose (red), and galactose (green). Conditions: T = 90°C, pH = 1.0, heterogeneous catalysts Smopex 101 and Amberlyst 15.

The leveling-off the manose, glucose, and galactose concentrations further confirm that at these conditions, formation of degradation products is minimal. Otherwise, one would expect that the concentrations of these monosaccharides would decrease as the time of reaction increases.

Homogeneous catalysis

The quantitative analysis of the experimental data was commenced by preparing the double logarithmic plots according to Eqs. 11 and 12. If the theory proposed previously is valid, the plots should be straight lines; they should be independent of pH and the acid catalyst used. Figures 7 and 8 reveal that the plots have this kind of behavior, except a small bending close to the origin, in the very beginning of the experiment. The plots demonstrate that the ratio of galactose-to-mannose and galactose-to-glucose formation is at the initial stage of the reaction higher, but decreases to a constant value as the reaction proceeds. This can be interpreted as follows: at the initial

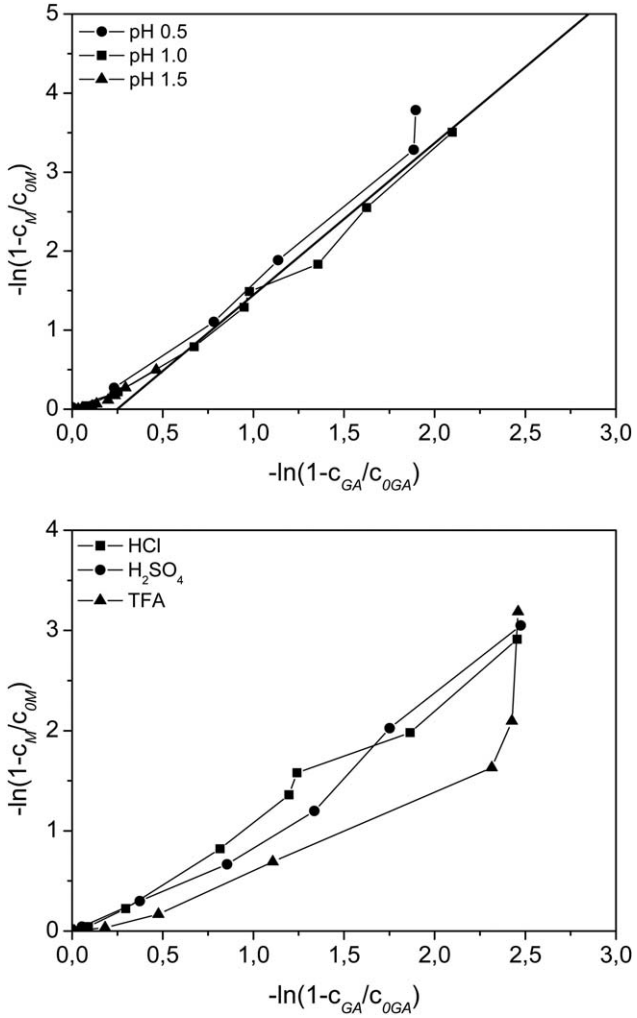

Figure 7. Logarithmic plots ln $(1 - c_M/c_{0M})$ vs. ln $(1 - c_{GA}/c_{0GA})$ for HCl (upper) and other catalysts (lower, pH = 1).

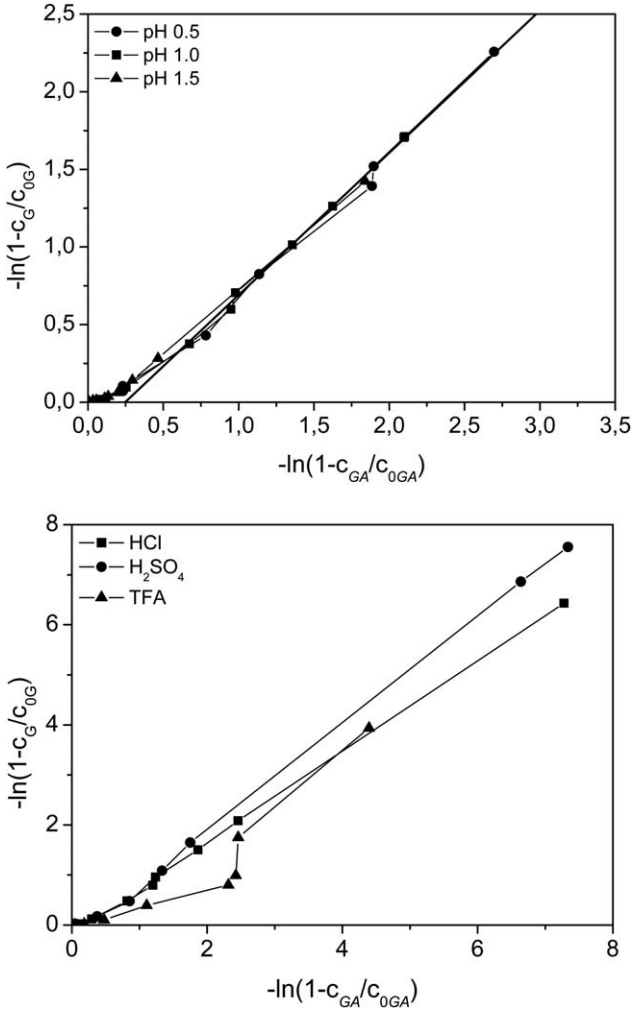

Figure 8. Logarithmic plots ln $(1 - c_G/c_{0G})$ vs. ln $(1 - c_{GA}/c_{0GA})$ for HCl (upper) and other catalysts (lower, pH = 1).

stage of the reaction, the galactose side chains are hydrolyzed more rapidly than the main chain of GGM. In general, the requirement that the plots are pH-independent and independent of the homogeneous acid catalyst used, is very well-fulfilled, as demonstrated by Figures 7 and 8.

The special case is an organic (trifluoroacetic) acid (TFA) which demonstrates some deviations from a linear trend (Figure 7). At the same time, the experimental points even for this acid are rather close to the ones for the mineral acids.

In fact, the deviations for TFA are because of the nature of the double logarithmic plot, when close to complete conversion there is a strong tendency for the logarithm to grow toward infinity.

Thus, in case of $-\ln(1 - c/c_0)$ for high values of c, as c approaches c_0 the function grows rapidly. Small experimental scattering can cause deviations from linearity.

From the slopes of the diagnostic plots, the reactivity ratio mannose-to-galactose and glucose-to-galactose can be roughly estimated. From Figures 7 and 8, the following values are obtained for the reactivity ratios at 90°C: 1.88 (mannose-to-galactose) and 0.86 (glucose-to-galactose). This means that the mannose units from the main chain are released most rapidly after the initial stage.

In the next stage, nonlinear regression analysis was applied to the kinetic data displayed in Figure 5. Because the effect of pH on the reaction rates was remarkably high, the data sets obtained at pH values 1.5, 1.0, and 0.5 were treated separately in the regression analysis. Preliminary tests with the data set recorded at pH = 1.5 revealed, that these data do not follow the model proposed, since the initiation period is quite long (Figure 5). The model including an autocatalytic contribution can describe the data set, as demonstrated by Figure 5. However, the reason for the autocatalysis, is not clear: it can be a real increase of the rate constant with conversion, but it can also be caused by oligomer formation. Therefore, the further effort was focused on the data sets representing pH = 0.5 and pH = 1.0. In these cases, a very satisfactory fit of the model was achieved, as demonstrated by Figure 5. The numerical values of the parameters along with the parameter estimation statistics are collected in Table 1. The parameters are well-defined, the standard errors are typically less than 20% and the degree of explanation exceeds 98%.

The Figures 5 and 6 showing the fit of model to experimental data also show the confidence interval (95%, gray area in the figures) for the model. For the calculation of the

Table 1. Parameter Estimation Results for the Homogeneous Catalyst (HCl) at 90°C

Parameter	Value	Std. Error	Std. Error (%)
pH = 0.5 (R^2 = 98.7%)			
$k_{01}c_H$/(L/mol/min)	0.787 10^{-3}	0.515 10^{-4}	15.3
$k_{02}c_H$/(L/mol/min)	0.552 10^{-3}	0.177 10^{-3}	3.1
$k_{03}c_H$/(L/mol/min)	0.253 10^{-3}	0.421 10^{-4}	6.0
pH = 1 (R^2 = 99.7%)			
$k_{01}c_H$/(L/mol/min)	0.725 10^{-3}	0.187 10^{-4}	38.8
$k_{02}c_H$/(L/mol/min)	0.626 10^{-3}	0.833 10^{-4}	7.5
$k_{03}c_H$/(L/mol/min)	0.473 10^{-3}	0.321 10^{-4}	14.7
pH = 1.5 (R^2 = 94.1%)			
$k_{01}c_H$/(L/mol/min)	0.303 10^{-3}	0.216 10^{-3}	14.0
$k_{02}c_H$/(L/mol/min)	0.341 10^{-3}	0.110 10^{-3}	3.1
$k_{03}c_H$/(L/mol/min)	0.228 10^{-3}	0.445 10^{-4}	5.1

k_1:mannose, k_2:galactose, k_3:glucose.

probability regions of the model, the Markov–Chain–Monte–Carlo method implemented in the software[36] was used.

The parameters obtained for pH = 0.5 and pH = 1.0 are in fairly good agreement. Thus, it can be concluded that the kinetic modelling principles presented in above can be applied to the hydrolysis of GGM in the presence of homogeneous acid catalysts at pH values 1 or less. For higher pH values, a more detailed chemical analysis of the oligomers formed is necessary for a further development of the kinetic approach.

Heterogeneous catalysis

The effects discovered for the heterogeneous catalysts (Smopex- 101 and Amberlyst 15) are interesting: both heterogeneous catalysts have a similar autocatalytic behavior, but Smopex is more active than Amberlyst (Figure 6). Difference between activity is even more profound when the number of acids sites is considered (3.6 m_{eq}/g for Smopex vs. 4.7 m_{eq}/g in case of Amberlyst). This can be explained by the fact that the active sites, that is the sulfonic acid groups, are better accessible for the Smopex catalyst, whereas most of them are "hidden" inside the pores of Amberlyst, and thus not accessible for the hemicellulose macromolecules. Similarly to the homogeneous catalyst, the galactose formation is slightly favored in the beginning of the reaction, but after an initiation period, the double logarithmic plots have a constant slope, as revealed by Figures 9 and 10. Moreover, the mannose-to-galactose and glucose-to-mannose ratios are the same for both catalysts, confirming that they behave chemically in a very similar manner.

The experimental data obtained for Smopex and Amberlyst were exposed to nonlinear regression analysis—the model Eq. 39 was used for galactose, glucose, and mannose. At the first stage, some preliminary estimation experiments were carried out by letting the parameter α vary. For instance, for Smopex an optimal value of about $\alpha = 0.7$ was determined by regression analysis. However, it turned out that an almost equally good description was achieved by setting α to 1 and estimating parameters k_{0i} and β only. In this way, only four parameters were estimated for each catalyst, by using three kinetic curves (Figure 6), which improved the estimation statistics, that is the errors of the parameters were suppressed. The parameter errors were typically less than 8% and the degree of explanation was 99.8 and 99.5% for Smopex and Amberlyst, respectively. The parameter values and the estimation statistics are summarized in Table 2 and the modeling results are displayed in Figure 6, which demonstrates the very good fit of the model to the experimental data. The α-value 1 implies that the rate constant increases linearly with decreasing *DP*. From a chemical viewpoint, this is expected: longer molecules have a lower reactivity, as has been shown, for instance for the reactions of carboxylic acids.[37] When an oligosaccharide is long enough the bonds can be assumed to have equal reactivity, while with a

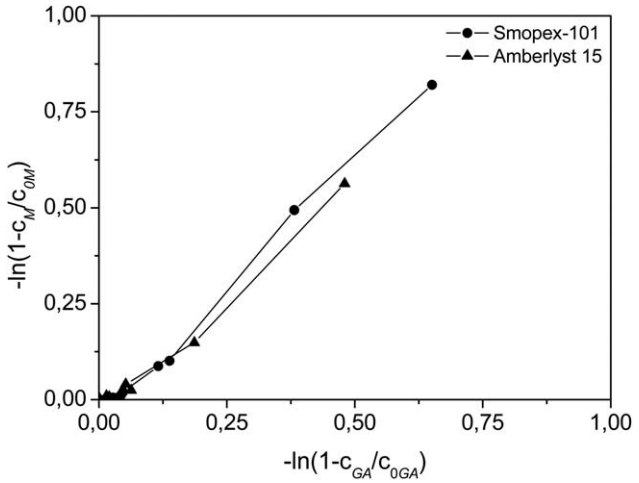

Figure 9. Logarithmic plots for heterogeneous catalysts: ln (1 − c_M/c_{0M}) vs. ln (1 − c_{GA}/c_{0GA}).

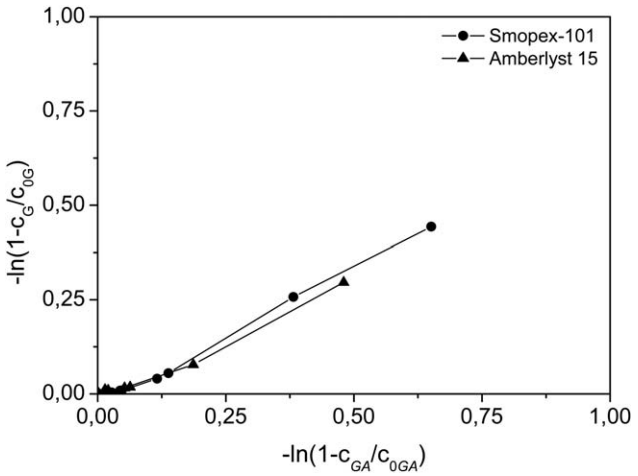

Figure 10. Logarithmic plots ln (1 − c_G/c_{0G}) vs. ln (1 − c_{GA}/c_{0GA}).

Table 2. Parameter Estimation Results for the Heterogeneous Catalysts at 90°C

Parameter	Value	Std. Error	Std. Error (%)
Smopex 101 ($R^2 = 99.99\%$)			
$k_{01}c_H\rho_B$/(L/mol/min)	$0.694\ 10^{-6}$	$0.109\ 10^{-7}$	6.3
$k_{02}c_H\rho_B$/(L/mol/min)	$0.721\ 10^{-6}$	$0.202\ 10^{-6}$	3.6
$k_{03}c_H\rho_B$/(L/mol/min)	$0.600\ 10^{-6}$	$0.137\ 10^{-6}$	4.4
β (dimensionless)	35.5	7.4	4.8
Amberlyst ($R^2 = 99.6\%$)			
$k_{01}c_H\rho_B$/(L/mol/min)	$0.194\ 10^{-6}$	$0.117\ 10^{-7}$	16.5
$k_{02}c_H\rho_B$/(L/mol/min)	$0.263\ 10^{-6}$	$0.467\ 10^{-7}$	5.6
$k_{03}c_H\rho_B$/(L/mol/min)	$0.172\ 10^{-6}$	$0.239\ 10^{-7}$	7.2
β (dimensionless)	125	7.4	11.5

k_1:mannose, k_2:galactose, k_3:glucose.

decrease of DP contribution of the terminal glycosidic bond with 1.8 higher reactivity[14] becomes more prominent.

Experimental data were not recorded for such a long reaction time that we could have been able to see the decline of the reaction rate at high conversions, that is at low concentrations of existing glycosidic bonds. However, a numerical simulation was carried out with the parameters obtained for Smopex 101. The simulation results are displayed in Figure 11, which reveals that the rate increases until 4000 min, which corresponds to the conversion level of $X = 50\%$ approximately (the inflexion points in the curves). Thereafter, the ordinary type of kinetics starts to dominate, as the concentrations of the reactive groups become lower and lower. To reach really high conversions, exceeding 90%, reaction times up to 10,000 min are needed as revealed by Figure 11. This is, however, not the final value, as there is room for process intensification: the catalyst bulk density can be increased (mass of catalyst-to-liquid volume ratio), catalyst acidity and what is even more important, somewhat higher experimental temperatures can be used. The thermal stability of the ion exchange resins, such as Amberlyst-15, is limited typically to about 120°C limiting the use of these catalysts. New solid hydrolysis catalysts with a better temperature resistance are under development, opening new avenues for heterogeneous catalytic hydrolysis of hemicellulose.

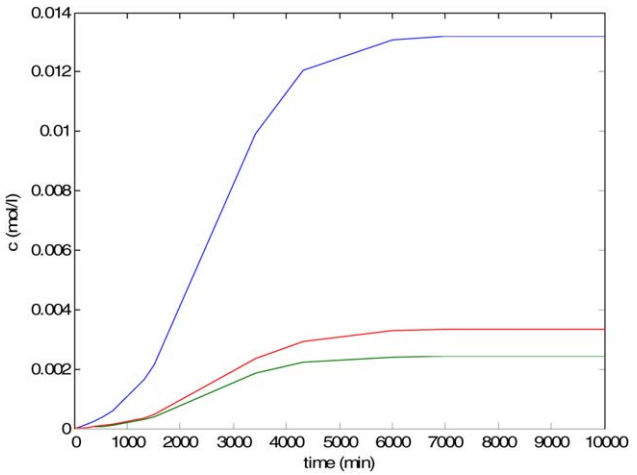

Figure 11. Simulation of the kinetics of GGM hydrolysis over heterogeneous catalyst (Smopex 101) at 90°C and pH = 1: mannose (blue), glucose (red), and galactose (green).

Kinetic parameters from Table 2. [Color figure can be viewed in the online issue, which is available at wileyonlinelibrary.com.]

Conclusions

Mathematical models were proposed for the hydrolysis of the hemicellulose GGM in the presence of homogeneous and heterogeneous acid catalysts. Although pentosan hydrolysis from hardwood and agricultural residues has been extensively studied typically at much higher temperatures resulting in formation of degradation products, hydrolysis of hemicelluloses from softwood (i.e., GGM) under milder temperatures (ca. 90°C) has attracted much less attention. However, this is an attractive way to obtain high-value sugar monomers from hemicelluloses. A new approach was applied to the autocatalytic kinetic phenomenon observed for heterogeneous catalysts, when hydrolysis of water-soluble oligosaccharides occurs at the surface of the solid materials. Autocatalysis was described with functions, which predicted the increase of the rate constant with increasing hemicellulose conversion and decreasing degree of polymerization. The models were able to describe the kinetic observations very well.

Acknowledgment

This work is part of the activities at the Åbo Akademi University Process Chemistry Centre within the Finnish Centre of Excellence programmes (2000–2011) appointed by the Academy of Finland and currently financed by Abo Akademi University.

Notation

A = proportionality constant, Eq. 21
c = concentration
D = diffusion coefficient
D_e = effective diffusion coefficient
DP = degree of polymerization
K = equilibrium constant
k = rate constant
k', k'' = modified rate constants
Q = objective function in regression analysis
R^2 = degree of explanation
t = time
X = conversion
α,α' = parameter
α_1 = parameter, Eq. 20
α_2 = parameter, Eq. 20
β, β' = parameter in autocatalysis
γ, γ' = exponent in kinetic model
ε = particle porosity
ρ_B = catalyst bulk density
τ = particle tortuosity
ω = parameter, Eq. 18

Subscripts

cat = catalyst
i,j = component indices referring to products
L = liquid phase

0 = initial state
$0i$ = total concentration of a sugar unit
$i0$ = concentration of unreacted sugar unit

Abbreviations

G = glucose
GA = galactose
GGM = *O*-acetylgalactoglucomannan
M = mannose
ODE = ordinary differential equation
W = water

Literature Cited

1. Mäki-Arvela P, Salmi T, Holmbom B, Willför S, Murzin DYu. Synthesis of sugars by hydrolysis of hemicelluloses: a review. *Chem Rev*. 2011;111:5638–5666.
2. Wyman CE, Decker SR, Himmel ME, Brady JW, Skopec CE, Viikari L. Hydrolysis of cellulose and hemicelluloses. In: Dumitriu S, editor. Polysaccharides: Structural Diversity and Functional Versatility, 2nd ed. New York: Marcel Dekker, Inc., 2004:995–1033.
3. Wyman C, Dale B, Elander R, Holzaplle M, Ladisch M, Lee Y, Mitchinson C, Saddler J. Comparative sugar recovery and fermentation data following pretreatment of poplar wood by leading technologies. *Biotechnol Prog*. 2008;25:333–339.
4. Kim Y, Hendrickson R, Mosier N, Ladisch MR. Plug-flow reactor for continuous hydrolysis of glucans and xylans from pretreated corn fiber. *Energy Fuels*. 2005;19:2189–2200.
5. Demma Cara P, Pagliaro M, Elmekawy A, Brown D R, Verschuren P, Shiju NR, Rothenberg G. Hemicellulose hydrolysis catalysed by solid acids. *Catal Sci Technol*. 2013;3:2057–2061.
6. Kusema BT, Hilpmann G, Mäki-Arvela P, Willför S, Holmbom B, Salmi T, Murzin DY. *Catal Lett*. 2011;141:408–412.
7. Guo F, Zhen F, Xu CC, Smith RJ Jr. Solid acid mediated hydrolysis of biomass for producing biofuels. *Prog Energy Combust Sci*. 2012; 38:672–690.
8. Huang YB, Fu Y. Hydrolysis of cellulose to glucose by solid acid catalysts. *Green Chem*. 2013;15:1095–1111.
9. Harris JF, Baker AJ, Conner AH, Jeffries TW, Minor JL, Pettersen RC, Scott RW, Springer EL, Wegner TH, Zerbe JI. Two-stage, dilute dulfuric acid hydrolysis of wood: an investigation of fundamentals. Forest Products Laboratory Report FPL-45. 1985, Madison, 1–73.
10. Ladisch MR. Hydrolysis. In: Biomass Handbook. London: Gordon and Breach, 1989;434–451.
11. Salmi T, Damlin P, Mikkola JP, Kangas M. Modelling and experimental verification of cellulose substitution kinetics. *Chem Eng Sci*. 2011;66:171–182.
12. Kobayashi T, Sakai V. Hydrolysis rate of pentosan of hardwood in dilute sulfuric acid. *Bull Agri Chem Soc Jpn*. 1956;20:1–7.
13. Maloney MT, Chapman TW, Baiker AJ. Dilute acid hydrolysis of paper birch-kinetic studies of xylan and acid group hydrolysis. *Biotechnol Bioeng*. 1985;27:355–361.
14. Kamiyama Y, Sakai Y. Rate of hydrolysis of xylo-oligosaccharides in dilute sulfuric acid. *Carbohydr Res*. 1979;73:151–158.
15. Gonzalez G, Lopez-Santin J, Caminal G, Sola S. Dilute acid hydrolysis of wheat straw hemicellulose at moderate temperature: a simplified kinetic model. *Biotechnol Bioeng*. 1986;18:288–293.
16. Chen R, Lee YY, Torget R. Kinetic and modeling investigation of two-stage reverse-flow reactor as applied to dilute-acid pretreatment of agricultural residue. *Appl Biochem Biotechnol*. 1996;57–58: 133–146.
17. Lavarack PB, Griffin GJ, Rodman D. The acid hydrolysis of sugarcane bagasse hemicellulose to produce xylose, arabinose, glucose and other products. *Biomass Bioenergy*. 2002;23:367–380.
18. Cahela DR, Lee YY, Chambers RP. Modelling of percolation process in hemicelluloses hydrolysis. *Biotechnol Bioenergy*. 1983;25:3–17.
19. Garrote G, Dominguez H, Parajo JC. Mild autohydrolysis: an environmentally friendly technology for xylooligosaccharide production from wood. *J Chem Technol Biotechnol*. 1999;74:1101–1109.
20. Garrote G, Dominguez H, Parajo JC. Kinetic modeling of corncob autohydrolysis. *Process Biochem*. 2001;36:571–578.
21. Jacobsen SE, Wyman CE. Cellulose and hemicelluloses hydrolysis models for application to current and novel pretreatment processes. *Appl Biochem Biotechnol*. 2000;84–86:81–96.
22. Xu C, Pranovich A, Vähäsalo L, Hemming J, Holmbom B, Schols HA, Willför S. Kinetics of acid hydrolysis of water-soluble spruce O-acetyl galactoglucomannans. *J Agri Food Chem*. 2008;56:2429–2435.
23. Kusema BT, Xu C, Mäki-Arvela P, Willför S, Holmbom B, Salmi T, Murzin DYu. Kinetics of acid hydrolysis of arabinogalactans. *Int J Chem React Eng*. 2010;8:A44 1–18.
24. Kusema B, Tönnov T, Mäki-Arvela P, Salmi T, Willför S, Holmbom B, Murzin D. Acid hydrolysis of O-acetylgalactoglucomannan. *Catal Sci Technol*. 2013;3:116–122.
25. Kumar R, Wyman CE. The impact of dilute sulfuric acid on the selectivity of xylooligomer depolymerization to monomers. *Carbohydr Res*. 2008;343:290–300. 26.
26. Kano Y, Sekine, Y. One pot direct catalytic conversion of cellulose to hydrocarbon by decarbonation using Pt/H-beta zeolite catalyst at low temperature. *Catal Lett*. 2013;143:418–423.
27. Patil SKR, Heltzel J, Lund CRF. Comparison of structural features of humans formed catalytically from glucose, fructose, and 5-hydroxymethylfurfuraldehyde. *Energy Fuels*. 2012;26:5281–5293.
28. Reyes-Luyanda D, Flores-Cruz J, Morales-Perez PJ, Encarnacion-Gomez LG, Shi F, Voyles PM, Cardona-Martinez N. Bifunctional materials for the catalytic conversion of cellulose into soluble renewable biorefinery feedstocks. *Top Catal*. 2012;55:148–161.
29. Sahu R, Dhepe PL. A one-pot method for the selective conversion of hemicellulose from crop waste into C5 sugars and furfural by using solid acid catalysts. *ChemSusChem*. 2012;5:751–761.
30. Dee SJ, Bell AT, A study of the acid-catalyzed hydrolysis of cellulose dissolved in ionic liquids and the factors influencing the dehydration of glucose and the formation of humans. *ChemSusChem*. 2011;4:1166–1173.
31. Kim Y, Kreke T, Ladisch MR. Reaction mechanisms and kinetics of xylo-oligosaccharide hydrolysis by dicarboxylic acids. *AIChE J*. 2013;59:188–199.
32. Salmi T, Mikkola JP, Wärnå J. Chemical Reaction Engineering and Reactor Technology. Boca Raton, FL: CRC Press Taylor & Francis Group, 2010.
33. Lilja J, Murzin DYu, Mäki-Arvela P, Salmi T, Sundell M. Esterification of different acids over heterogeneous and homogeneous catalysts and correlation with the Taft equation. *J Mol Catal A*. 2002; 182-183:555–563.
34. Bienkowski PR, Ladisch MR, Narayan R, Tsao GT, Eckert R. Correlation of cluvose (dextrose) degradation at 90 to 190 oc in 0.4 to 20% acid. *Chem Eng Commun*. 1987;51:179–192.
35. Willför S, Rehn P, Sundberg A, Sundberg K, Holmbom B. Recovery of water-soluble acetyl-galactoglucomannans from mechanical pulp of spruce *Tappi J*. 2003;2:27–32.
36. Haario H. ModEst: User's Guide. Helsinki: Profmath Oy, 2007.
37. Paatero E, Salmi T, Fagerstolt K. Selective synthesis of α-chlorocarboxylic acids. *Ind Eng Chem Res*. 1992;31:2426–2437.

Manuscript received July 31, 2013, and revision received Nov. 7, 2013.